A Thesis for the Degree of Master of Science

Coumestrol, a component of soybean sprout, attenuates UVB-induced skin photoaging by targeting FLT3

자외선에 의한 FLT3 활성 저해를 통한 쿠메스트롤의 피부노화 개선효능 및 작용기작 규명

By

Gaeun Park

Department of Agricultural Biotechnology

Seoul National University

August, 2014

석사학위논문

Coumestrol, a component of soybean sprout, attenuates UVB-induced skin photoaging by targeting FLT3

자외선에 의한 FLT3 활성 저해를 통한 쿠메스트롤의 피부노화 개선효능 및 작용기작 규명

지도교수 이 기 원

이 논문을 석사학위 논문으로 제출함

2014년 8월

서울대학교 대학원

농생명공학부

박가은

박가은의 석사학위논문을 인준함

2014년 8월

위 원 장 강 동 현 (인)

부위원장 이 기 원 (인)

위 원 하 남 출 (인)

Abstract

Skin aging is a naturally occurring process by senescence. However, exposure to ultraviolet (UV) light triggers wrinkle formation and sagging of skin due to collagen degradation by activating matrix metalloproteinases (MMPs). In this study, I show that coumestrol, a metabolite of soybean isoflavone daidzein, has stronger preventive effect on skin photoaging than daidzin and daidzein in three-dimensional human skin equivalent model. The results showed that coumestrol inhibits UVB-induced MMP-1 activity and MMP-1 expression. To identify a direct molecular target of coumestrol, whole human kinase profiling assay was conducted and FLT3 kinase was proposed as a novel target protein of coumestrol in UVB-induced signaling pathway in skin. Coumestrol suppresses FLT3 kinase activity, and subsequently, Ras/MEK/ERK and Akt/p70S6K pathway. This led to the suppressed AP-1 activity and in turn, diminished MMP-1 gene transcription by coumestrol. 4-APIA, pharmacological inhibitor of FLT3, inhibited MMP-1 expression and induced similar signal

transduction changes with coumestrol. Taken together, coumestrol inhibits UVB-induced MMP-1 expression by suppressing FLT3 kinase activity. This finding suggests that coumestrol is a novel dietary compound with potential utilization in preventing and improving UVB-associated skin aging.

Keywords: Coumestrol; FLT3; MMP-1; UVB

Student ID: 2012-23375

Contents

I. Introduction

Skin aging is a naturally occurring process by senescence and has clinical signs such as fine wrinkles, pale, sagging [1, 2]. During the aging, skin, especially face, neck, and hand, is easy to be affected by additional damage such as sunlight, air pollution, xenobiotics, and extreme temperature and that makes premature skin aging [2, 3]. In particular, sunlight is the major cause of worsening appearance of aged skin, for instance about 80 % of facial skin aging is attributable to sunlight [4]. Sun-exposed skin features deep wrinkles, dry, uneven pigmentation, and an accelerated decline in the function of skin [2, 3, 5].

Sunlight is divided into ultraviolet (UV), infra-red (IR), and visible light based on wavelengths. Among them, UV plays an important role in skin aging. UV comprises UVA (320 ~ 400 nm), UVB (280 ~ 320 nm), and UVC (200 ~ 280 nm). Since UVC is blocked by Ozone layer, UVA and UVB are an actual cause of skin aging [6, 7]. UVB contain more energy than UVA and the radiation leads to skin damage such as sunburn, suntanning, immune-

suppression, photoaging [7], and photo-carcinogenesis [8].

Exposure to UVB alters biological processes that promote matrix metalloproteinases (MMPs) expression, decrease procollagen synthesis, and increase connective tissue damage [3, 9, 10]. These complex changes trigger wrinkle formation throughout various layer of the skin, but the major changes are seen in the dermis [11, 12]. MMP-1 is a type of collagenase, and it breaks down collagen fibrils. Repeated UVB exposure increases the level of MMP-1 in the dermis and dermal fibroblasts, therefore triggers histopathological changes and clinical manifestations [9, 10, 12]. MMP-1 expression is mediated by cellular signaling transduction such as mitogen-activated protein kinase (MAPK) and phosphatidylinositol 3-kinase (PI3K)/Akt [13, 14]. These signaling cascades elevate activator protein 1 (AP-1) activity and enhance MMP-1 gene transcription.

Coumestrol (Fig 1), one of the soybean isoflavonoids, belongs to coumestans family [15, 16]. Under stress such as germination or fungal infection, chemical elicitors, coumestrol is

made from daidzein through *de novo* synthesis as a soybean phytoalexin [17, 18]. Therefore, it is commonly found in soybean leaves, bean sprouts, alfafa and so on [15, 19]. Coumestrol has higher antioxidant activity than daidzein and genistein which are the major soybean isoflavone secondary metabolites [20, 21]. However, most of studies about soybean isoflavonoids focus on isoflavones. Recent reports showed that coumestrol exerts anti-cancer, anti-obesity, and neuroprotection effects [22-24]. However, the effect of coumestrol on skin aging has not yet been studied. In this study, I investigated the effect of coumestrol on UVB-induced MMP-1 expression to uncover coumestrol's potential protective effect against skin photoaging.

Ⅱ. Materials and Methods

2.1. Chemicals and reagents

Coumestrol, dadizin, daidzein, fetal bovine serum (FBS), and β-actin antibody were obtained from Sigma-Aldrich (St.Louis, MO). Dulbecco's modified eagle medium (DMEM) was purchased from Hycolne (Long, UT). The MMP-1 antibody was obtained from R&D Systems Inc. (Minneapolis, MN). Antibodies against phosphorylated extracellular-signal regulated kinase 1/2 (ERK1/2) (Thr^{202}/Ty^{r204}) and total ERK1/2 were purchased from Santa Cruz Biotechnology (Santa Cruz, CA). The other antibodies were obtained from Cell Signaling Biotechnology (Beverly, MA). The CellTiter-Glo luminescent cell viability assay was purchased from Promega Corporation (Madison, WI). Penicillin/streptomycin was purchased from Life technologies (Carlsbad, CA). Protein assay kits were obtained from Bio-Rad Laboratories (Hercules, CA). 4-(4-Aminophenyl)-1H-indazol-3-ylamine (3-aminoindazole compound) was obtained from MERCK Millipore (Nottingham, UK).

2.2. Cell culture and UVB irradiation

Primary human dermal fibroblasts (HDFs) were isolated from the outgrowth of foreskin obtained from 7 to 30 year old healthy volunteers from Dr. Chung JH laboratory (Seoul National University Hospital, Korea) under the Institutional Review Board at Seoul National University Hospital and Seoul National University. HDFs were cultured in DMEM with 10 % (v/v) FBS and 1 % (v/v) penicillin/streptomycin at 37 ℃ and 5 % CO_2. UVB irradiation was performed on serum-starved monolayer cultures. HDFs were exposed to UVB at a dose of 0.02 J/cm^2 using UVB source (Bio-Link crosslinker, VilberLourmat, Cedex 1, France) set spectral peak at 312 nm.

2.3. Three dimensional (3D) human skin equivalent

Using Neoderm®-ED purchased from TEGO Science (Seoul, Korea), I made the 3D human skin equivalent. Briefly, HDFs were cultured in the collagen matrix for 1 day. And then keratinocyte were seeded on top of collagen matrix and co-cultured

for 4 days. Next, lifted the keratinocytes and HDF block to expose the air. And 20 μM of coumestrol, daidzin, and daidzein were treated for 1 h after 2 weeks of the air-lift. After that, 3D human skin blocks were irradiated 0.05 J/cm^2 UVB twice a day for 8 days. During 8 days, medium was changed every 2 days, and blocks are incubated at 37 ℃ and 5 % CO_2.

2.4. Cell viability

The cell viability was measured using the CellTiter-Glo luminescent cell viability assay (Promega) followed by manufacturer's instructions.

2.5. Histological examination

To evaluate collagen in the dermis, 3D human skin blocks were fixed with 10 % neutral-buffered formalin, and embedded in paraffin. I sectioned the 3D human skin paraffin block (4 μm thickness) and transferred onto slides. After deparaffinizing, skin

block sections were stained with Hematoxylin for 5 min. And then, slides were washed and stained in biebrich scarlet and acid fuchsin. Next, place the slides in phosphomolybdic-phosphotungstic acid for 10 min and aniline blue for 5 min to stain collagen. Slides were then washed and incubated in 1 % acetic acid for 15 min. Lastly, dehydrate and wash. Skin block sections were examined at 400× magnification using an Olympus AX70 light microscope (Tokyo, Japan).

2.6. Immunohistochemical staining

To measure the level of MMP-1, 3D human skin equbanlet blocks were fixed, embedded, and deparaffinized as described above. Slides were incubated in 0.3 % hydrogen peroxide to remove the endogenous peroxidases and blocked using 5 % normal goat serum for 30 min. After blocking, slides were incubated with MMP-1 antibody (R&D Systems Inc.) at 4 ℃ overnight. Next, they were reacted to biotinylated secondary antibody (Vector Labs, Burlingame, CA) and developed using avidin-biotin complex kit

(Vector Labs). The reaction was visualized with 3,3'-diaminobenzidine tetrahydrochloride hydrate solution (Vector Labs). And the counterstain was conducted using hematoxylin. The level of MMP-1 in 3D human skin block was examined under 400× magnification using an Olympus AX70 light microscope.

2.7. Enzyme-linked immunosorbent assay (ELISA)

To determine MMP-1 contents in the conditioned medium of HDFs, the DuoSet human total MMP-1 ELISA kit (R&D system Inc.) was used according to the manufacturer's instructions.

2.8. MMP-1 activity assay

MMP-1 activity was measured by using SensoLyte 520 MMP-1 assay kit (AnaSpec Inc., USA) according to the manufacturer's instructions. Briefly, upon cleavage into two separate fragments (5-FAM and QXL^{TM} 520) by activated MMP-1, the fluorescence of 5-FAM was recovered, and could be monitored

at excitation/emission (490/520 nm). The change of enzyme activity of MMP-1 was presented as percent change in relative fluorescence unit versus control.

2.9. Real-time RT-PCR

HDFs were treated with coumestrol for 12 h and harvested in RNAiso Plus (Takara Bio Inc., Shiga, Japan). After RT with oligo-dT primers using a PrimeScript^{TM} 1st strand cDNA synthesis Kit (Takara Bio Inc.), Real-time quantitative RT-PCR was performed using IQ SYBR (Bio-Rad Laboratories) using 2 μl of cDNA in triplicate with Glyceraldehyde 3-phosphate dehydrogenase (GAPDH) as internal control. The PCR parameters were 95 ℃ for 10 min, 40 cycles at 95 ℃ for 15 sec, 60 ℃ for 1 min, and 72 ℃ for 30 sec. Side-strand-specific primers for MMP-1, GAPDH were as follows: MMP-1 forward (5'-CCC CAA AAG CGT GTG ACA GTA-3'); MMP-1 reverse (5'-GGT AGA AGG GAT TTG TGC G-3'); GAPDH forward (5'-GAG TCA ACG GAT TTG GTC GT-3'); GAPDH reverse (5'-TTG ATT TTG GAG GGA TCT CG-3').

2.10. AP-1 reporter gene assay

HDFs were cultured for 16 h and co-transfected with 0.5 μg of Renilla vector, 5 μg of luciferase gene expression vectors containing AP-1 binding sequences (TGAC/GTCA) by JetPEI (Polylus, France). After 9 h of transfection, medium was changed with DMEM-10 % FBS for 15 h, and then starved in serum-free DMEM for 24 h. After starvation, the cells were treated with or without various concentrations of coumestrol for 1 h, followed by 0.02 J/cm^2 UVB irradiation. Cell extracts were prepared with reporter lysis buffer (Promega), and the extracts were used for luciferase assay. AP-1 activity in HDFs was determined by using an AP-1 luciferase assay kit (Promega), as described by the manufacturers. The ratio of firefly luciferase activity to Renilla luciferase activity in each sample served as a measure of normalized luciferase activity and transfection efficiency.

2.11. Western blot analysis

HDFs were cultured for 48 h, and then the cells were incubated in serum-free DMEM for 24 h. After that, the cells were treated with or without various concentrations of coumestrol (5, 10 and 20 μM) or daidzin (20 μM), daidzein (20 μM) for 1 h, followed by UVB (0.02 J/cm^2) irradiation. The cells were lysed using RIPA Lysis buffer (Cell signaling) on ice, scraped and then centrifuged at 18,620 ×g for 10 min. The protein concentration was measured using a dye-binding protein assay kit (Bio-Rad Laboratories) as described by the manufacturer. The proteins were separated electrophoritically using a 10 % SDS-polyacrylamide gel and transferred onto an Immobilon P membrane (MERK Millipore). The membrane was blocked in 5 % fat-free milk for 1 h, and then incubated with the specific primary antibody at 4 °C overnight. Protein bands were visualized using a chemiluminescence detection kit (GE healthcare, London, UK) after hybridization with the HRP-conjugated secondary antibody (Life technologies).

2.12. Zymography

Zymography was performed in 12 % polyacrylamide gels in the presence of gelatin (0.1 % w/v) as a substrate for MMP-2. The supernatants mixed with loading buffer [10 % SDS, 25 % glycerol, 0.25 M Tris (pH 6.8) and 0.1 % bromophenol blue], and the run on 12 % SDS-PAGE gels without denaturation. Afterward, the gelatin gels were washed with renaturating buffer (Life technologies) for 1 h at room temperature and incubated for 24 h at 37 °C in developing buffer (Life technologies). After enzyme reaction, the gelatin gels were stained with 0.5 % Coomassie brilliant blue in 10 % Acetic acid and then washed out using destaining buffer for 10 min.

2.13. Kinase profiling analysis and kinase assay

Kinase profiling analysis was conducted by KinaseProfiler^{TM} service (MERCK Millipore). The analysis was

followed manufactur's protocol. Briefly, FLT3 (h) is incubated with 50 mM Tirs/HCl pH 7.5, 150 mM NaCl, 0.1 mM EGTA, 0.03 % Triton X-100, 270 mM sucrose, 1 mM benzamidine, 0.2 mM PMSF, 0.1 % 2-mercaptoethanol, 100 μM Abltide (EAIYAAPFAKKK), 10 mM MgAcetate and [γ-33P-ATP]. The reaction was initiated by the addition of the MgATP mix. After incubation for 10 min at 30 °C, the reaction was stopped by the addition of 3 % phosphoric acid solution. 10 μl of the reaction was then spotted onto a P30 filtermat and washed three times for 5 min in 75 mM phosphoric acid and once in methanol for 2 min prior to drying and scintillation counting.

2.14. Statistical analysis

Data was expressed as the means ± standard deviation (S.D.). One-way analysis of variance (ANOVA) with Tukey's HSD test was used to evaluate mean differences of group and statistical significance. Differences were considered significant at $p < 0.05$.

Ⅲ. Results

3.1. Coumestrol inhibits UVB-induced collagen degradation and collagenase expression in 3D human skin equivalent.

To investigate the anti-wrinkle effect of coumestrol, I examined the effect of coumestrol collagen fibrils and collagenase (MMP-1) in 3D human skin culture system as described Fig. 2A. After 8 days of UVB irradiation in the presence or absence of coumestrol, paraffin-embedded 3D human skin tissues were sectioned and subjected to Masson's trichrome stain and immunohistochemistry. Coumestrol inhibited UVB-induced collagen degradation and MMP-1 expression at 20 μM, while daidzin and dzidzein had less effect (Fig. 2B and C). Taken together, I recognized that coumestrol had better preventive effect on photoaging than its precursor (daidzin and daidzein).

Figure 1

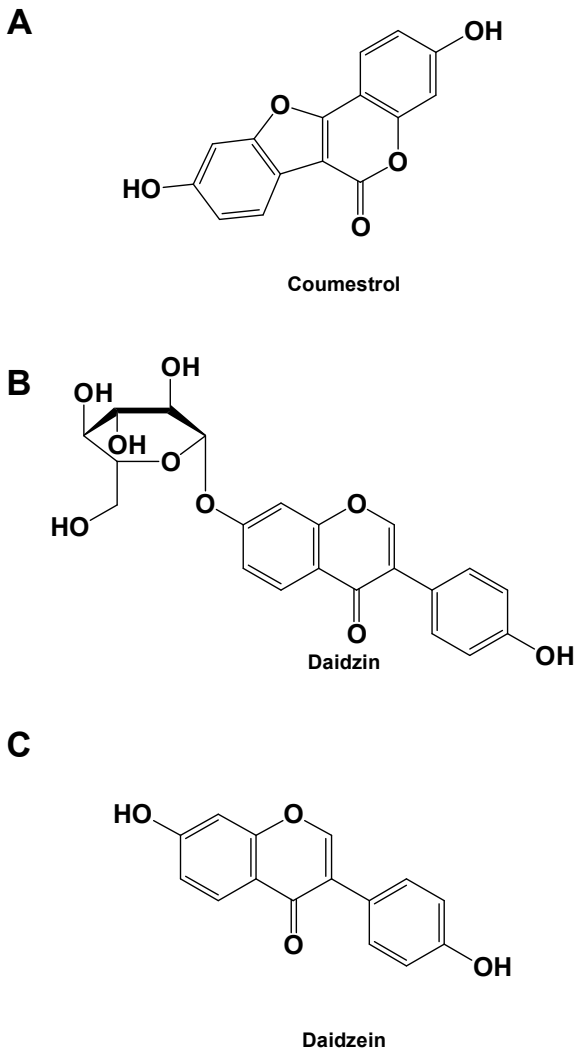

Figure 1. Chemical structure of coumestrol, daidzin, and daidzein

Figure 2

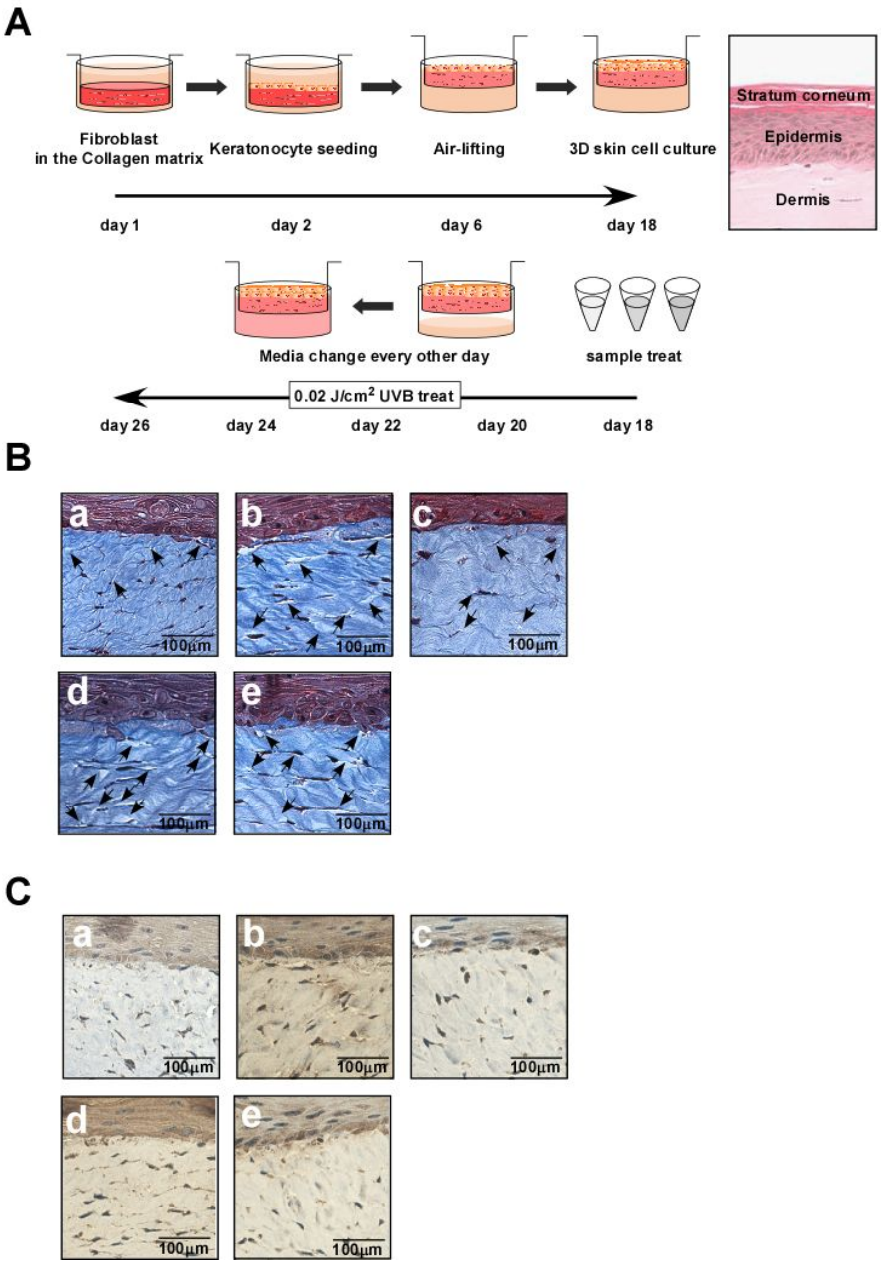
A
Fibroblast
in the Collagen matrix
Keratonocyte seeding
Air-lifting
3D skin cell culture
Stratum corneum
Epidermis
Dermis
day 1
day 2
day 6
day 18
Media change every other day
sample treat
0.02 J/cm2 UVB treat
day 26
day 24
day 22
day 20
day 18
B
a
b
c
d
e
100μm
C
a
b
c
d
e
100μm

Figure 2. Effect of coumestrol on UVB-induced collagen degradation and MMP-1 expression in 3D human skin equivalent.

A, A schematic diagram of 3D human skin cell culture system. The experiment process was described in materials and methods. **B**, Representative histological analysis of section of 3D human skin block treated with coumestrol, daidzin, and daidzein (20 μM). Masson's trichrome staining was used to identify collagen fibrils. The arrows indicate degraded collagen (400×, Scale bar 100 μm): untreated control (a); UVB (0.05 J/cm^2) only (b); UVB and coumestrol (c); UVB and daidzin (d); UVB and daidzein (e). **C**, The level of MMP-1 in 3D human skin block was measured using immunohistochemical staining (400×, Scale bar 100 μm): untreated control (a); UVB (0.05 J/cm^2) only (b); UVB and coumestrol (c); UVB and daidzin (d); UVB and daidzein (e).

3.2. Coumestrol suppresses UVB-induced MMP-1 activity by modulating MMP-1 expression.

To investigate that how coumestrol prevent collagen degradation, I measured enzyme activity and protein expression levels of MMP-1 using HDFs. Coumestrol (50 ± 0.4 %) significantly decreased MMP-1 activity compared with the UVB-irradiated (100 ± 1 %) and its precursor (daidzin 71 ± 0.8 % and daidzein 64 ± 1 %) groups (Fig. 3A). Coumestrol markedly reduced UVB-induced MMP-1 protein expression (UVB-irradiated group 38 ± 0.5 ng/ml) in a concentration-dependent manner at 5 μM (29.2 ± 0.5 ng/ml), 10 μM (14.9 ± 0.6 ng/ml), and 20 μM (4.5 ± 0.1 ng/ml), and exhibited better inhibitory effect than daidzin and daidzein (Fig. 3B and C) within the concentrations which did not affect cell viability (Fig. 3D). Overall, these results represented that coumestrol modulated MMP-1 activity through reducing UVB-induced MMP-1 expression.

Figure 3

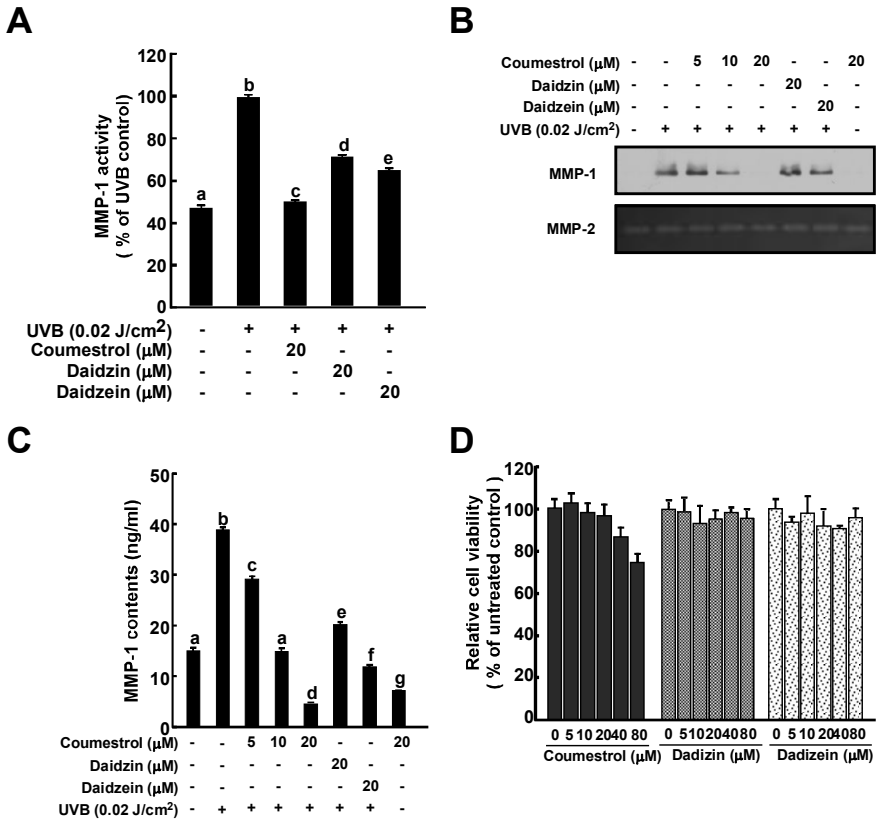

Figure 3. Effect of coumestrol on UVB-induced MMP-1 activity.

A, The level of MMP-1 activity was measured using SensoLyte 520 MMP-1 assay kit (AnaSpec Inc.) after 48 h UVB exposure. Data are the means ± SD (n = 3). Means with letters (a-e) within a graph were significantly different from each other at $p < 0.05$. **B**,

Expression of MMP-1 was determined by Western blotting as described at Materials and Methods. MMP-2 was used as loading control. (Can you improve the image quality of MMP-2 band by adjusting brightness and contrast etc.?) Data were representative of three independent experiments that yield similar result. **C**, The level of MMP-1 was quantified using an ELISA as described in the Materials and Methods. Data were the means ± S.D. (n = 3). Means with letters (a-g) within a graph were significantly different from each other at $p < 0.05$. **D**, Cell viability of coumestrol, daidzin, and daidzein. The viability was measured using the CellTiter-Glo luminescent cell viability assay (Promega) as described in the Materials and Methods. Data were shown as the means ± S.D. of three independent experiments.

3.3. Coumestrol reduces the FLT3 kinase activity.

To find a direct target protein of coumestrol in early time of UVB signaling pathway, Kinase profiling analysis was conducted by KinaseProfiler^{TM} service (MERCK Millipore). First, 356 kinases activities were analyzed with 40 μM coumestrol (Table 1). Based on Table 1, I selected 65 kinases whose activities were inhibited more than 80 %. KinaseProfiler^{TM} service was carried out again with selected kinases with 5 μM of coumestrol (Table 2). I selected the kinases which expressed in human skin using protein atlas database [25]. To verify kinase profiling assay data, I did *in vitro* FLT3 kinase assay and revealed that coumestrol drastically decreased FLT3 kinase activity (IC_{50} = 938 nM) (Fig. 4).

Table 1

Table 1. Kinase screening of coumestrol (40 μM)

Kinase profiling analysis was performed on whole human kinases (356 kinases) to find the target of coumestrol (40 μM) by KinaseProfiler™ service (MERCK Millipore). Data were representative of two independent experiments that gave similar results.

Kinase	Activity	Kinase	Activity	Kinase	Activity	Kinase	Activity	Kinase	Activity
Abl(h)	50	AMPKα2(h)	10	Axl(h)	42	BTK(h)	10	CaMKIIδ(h)	30
ACK1(h)	38	ARK5(h)	47	Blk(h)	11	B-Raf(h)	25	CaMKIV(h)	68
ALK(h)	17	ASK1(h)	84	Bmx(h)	41	CaMKI(h)	49	CDK1/cyclinB(h)	36
ALK4(h)	65	Aurora-A(h)	5	BRK(h)	58	CaMKIIβ(h)	22	CDK2/cyclinA(h)	32
Arg(h)	67	Aurora-B(h)	5	BrSK1(h)	6	CaMKIIγ(h)	20	CDK2/cyclinE(h)	33
AMPKα1(h)	26	Aurora-C(h)	22	BrSK2(h)	8	CaMKIδ(h)	40	CDK3/cyclinE(h)	33

Table 1. continue

Kinase	Activity	Kinase	Activity	Kinase	Activity	Kinase	Activity	Kinase	Activity
CDK5/p25(h)	25	CK2α2(h)	2	DDR2(h)	93	EphA8(h)	57	FGFR4(h)	66
CDK5/p35(h)	37	CLK1(h)	1	DMPK(h)	77	EphB2(h)	53	Fgr(h)	22
CDK6/cyclinD3(h)	36	CLK2(h)	2	DRAK1(h)	10	EphB1(h)	37	Flt1(h)	10
CDK7/cyclinH/MAT1(h)	86	CLK3(h)	24	DYRK2(h)	-3	EphB3(h)	91	Flt3(h)	5
CDK9/cyclin T1(h)	27	CLK4(h)	3	eEF-2K(h)	64	EphB4(h)	70	Flt4(h)	3
CHK1(h)	43	cKit(h)	17	EGFR(h)	73	ErbB4(h)	58	Fms(h)	59
CHK2(h)	17	CSK(h)	75	EphA1(h)	61	FAK(h)	67	Fyn(h)	22
CK1γ1(h)	22	c-RAF(h)	24	EphA2(h)	44	Fer(h)	66	GCK(h)	4
CK1γ2(h)	17	cSRC(h)	50	EphA3(h)	52	Fes(h)	50	GCN2(h)	81
CK1γ3(h)	6	DAPK1(h)	37	EphA4(h)	79	FGFR1(h)	10	GRK1(h)	83
CK1δ(h)	4	DAPK2(h)	25	EphA5(h)	75	FGFR2(h)	34	GRK5(h)	74
CK2(h)	-1	DCAMKL2(h)	72	EphA7(h)	57	FGFR3(h)	49	GRK6(h)	82

Table 1. continue

Kinase	Activity	Kinase	Activity	Kinase	Activity	Kinase	Activity	Kinase	Activity
GRK7(h)	72	IKKβ(h)	54	JNK1α1(h)	81	MAPK2(h)	45	MLK1(h)	10
GSK3α(h)	5	IKKε(h)	48	JNK2α2(h)	91	MAPKAP-K2(h)	58	Mnk2(h)	1
GSK3β(h)	4	IR(h)	70	JNK3(h)	28	MAPKAP-K3(h)	76	MRCKα(h)	77
Haspin(h)	2	IR(h), activated	46	KDR(h)	5	MEK1(h)	76	MRCKβ(h)	65
Hck(h)	8	IRE1(h)	86	Lck(h)	31	MARK1(h)	67	MSK1(h)	26
Hck(h) activated	11	IRR(h)	14	Lck(h)activated	31	MELK(h)	28	MSK2(h)	8
HIPK1(h)	15	IRAK1(h)	38	LIMK1(h)	58	Mer(h)	16	MSSK1(h)	33
HIPK2(h)	6	IRAK4(h)	21	LKB1(h)	67	Met(h)	29	MST1(h)	32
HIPK3(h)	6	Itk(h)	52	LOK(h)	20	MINK(h)	15	MST2(h)	4
IGF-1R(h)	65	JAK1(h)	43	Lyn(h)	12	MKK6(h)	123	MST3(h)	31
IGF-1R(h), activated	52	JAK2(h)	49	LRRK2(h)	91	MKK7β(h)	84	MST4(h)	46
IKKα(h)	69	JAK3(h)	16	MAPK1(h)	72	MLCK(h)	18	mTOR(h)	82

Table 1. continue

Kinase	Activity	Kinase	Activity	Kinase	Activity	Kinase	Activity	Kinase	Activity
mTOR/FKBP12(h)	65	PAK4(h)	67	Pim-3(h)	6	PKCι(h)	91	PTK5(h)	28
MuSK(h)	57	PAK5(h)	34	PKA(h)	57	PKCμ(h)	42	Pyk2(h)	38
NEK2(h)	87	PAK6(h)	48	PKBα(h)	52	PKCθ(h)	68	Ret(h)	5
NEK3(h)	76	PAR-1Bα(h)	43	PKBβ(h)	44	PKCζ(h)	69	RIPK2(h)	7
NEK6(h)	30	PASK(h)	9	PKBγ(h)	18	PKD2(h)	25	ROCK-I(h)	57
NEK7(h)	60	PEK(h)	77	PKCα(h)	80	PKG1α(h)	13	ROCK-II(h)	25
NEK9(h)	11	PDGFRα(h)	39	PKCβI(h)	84	PKG1β(h)	13	Ron(h)	45
NEK11(h)	32	PDGFRβ(h)	53	PKCβII(h)	89	Plk1(h)	58	Ros(h)	89
NLK(h)	18	PDK1(h)	33	PKCγ(h)	80	Plk3(h)	33	Rse(h)	61
p70S6K(h)	9	PhKγ2(h)	19	PKCδ(h)	79	PRAK(h)	26	Rsk1(h)	15
PAK1(h)	46	Pim-1(h)	1	PKCε(h)	95	PRK2(h)	37	Rsk2(h)	19
PAK2(h)	70	Pim-2(h)	9	PKCη(h)	86	PrKX(h)	44	Rsk3(h)	46

Table 1. continue

Kinase	Activity	Kinase	Activity	Kinase	Activity	Kinase	Activity	Kinase	Activity
Rsk4(h)	35	SRPK1(h)	60	Tec(h) activated	27	TYK2(h)	25	PI3 Kinase (p110β/p85α)(h)	79
SAPK2a(h)	99	SRPK2(h)	82	TGFBR1(h)	90	ULK2(h)	74	PI3 Kinase (p120γ)(h)	79
SAPK2b(h)	78	STK25(h)	82	Tie2 (h)	38	ULK3(h)	67	PI3 Kinase (p110δ/p85α)(h)	78
SAPK3(h)	62	STK33(h)	22	TLK2(h)	75	Wee1(h)	78	PI3 Kinase (p110α/p85α)(h)	75
SAPK4(h)	61	Syk(h)	33	TrkA(h)	13	WNK2(h)	42	PI3KC2α(h)	87
SGK(h)	19	TAK1(h)	46	TrkB(h)	30	WNK3(h)	60	PI3KC2γ(h)	44
SGK2(h)	30	TAO1(h)	23	TrkC(h)	17	VRK2(h)	68	PIP4K2α(h)	89
SGK3(h)	14	TAO2(h)	26	TSSK1(h)	27	Yes(h)	23	PIP5K1α(h)	70
SIK(h)	46	TAO3(h)	38	TSSK2(h)	35	ZAP-70(h)	86	PIP5K1γ(h)	88
Snk(h)	34	TBK1(h)	58	Txk(h)	40	ZIPK(h)	21		

Table 2

Table 2. Kinase screening of coumestrol (5 μM)

65 kinases were selected by criteria, an effect of inhibiting more than 80 % kinase activity, based on Table 1. And then, kinase profiling analysis conducted one more. Data were representative of two independent experiments that yielded similar results.

Kinase	Activity	Kinase	Activity	Kinase	Activity	Kinase	Activity	Kinase	Activity
ALK(h)	59	BrSK2(h)	50	CK1δ(h)	27	cKit(h)	32	Flt4(h)	8
AMPKα2(h)	78	BTK(h)	67	CK2(h)	5	DRAK1(h)	45	GCK(h)	13
Aurora-A(h)	68	CaMKIIγ(h)	61	CK2α2(h)	14	DYRK2(h)	16	GSK3α(h)	14
Aurora-B(h)	35	CHK2(h)	67	CLK1(h)	10	FGFR1(h)	77	GSK3β(h)	30
Blk(h)	85	CK1γ2(h)	67	CLK2(h)	24	Flt1(h)	32	Haspin(h)	3
BrSK1(h)	42	CK1γ3(h)	74	CLK4(h)	6	Flt3(h)	13	Hck(h)	67

Table 2. continue

Kinase	Activity	Kinase	Activity	Kinase	Activity	Kinase	Activity	Kinase	Activity
Hck(h) activated	47	LOK(h)	79	MSK2(h)	78	Pim-1(h)	16	RIPK2(h)	18
HIPK1(h)	43	Lyn(h)	71	MST2(h)	41	Pim-2(h)	56	Rsk1(h)	61
HIPK2(h)	38	Mer(h)	48	NEK9(h)	83	Pim-3(h)	36	Rsk2(h)	80
HIPK3(h)	46	MINK(h)	41	NLK(h)	46	PKBγ(h)	99	SGK(h)	95
IRR(h)	30	MLCK(h)	43	p70S6K(h)	58	PKG1α(h)	41	SGK3(h)	103
JAK3(h)	99	MLK1(h)	57	PASK(h)	53	PKG1β(h)	48	TrkA(h)	30
KDR(h)	20	Mnk2(h)	9	PhKγ2(h)	70	Ret(h)	41	TrkC(h)	81

Figure 4

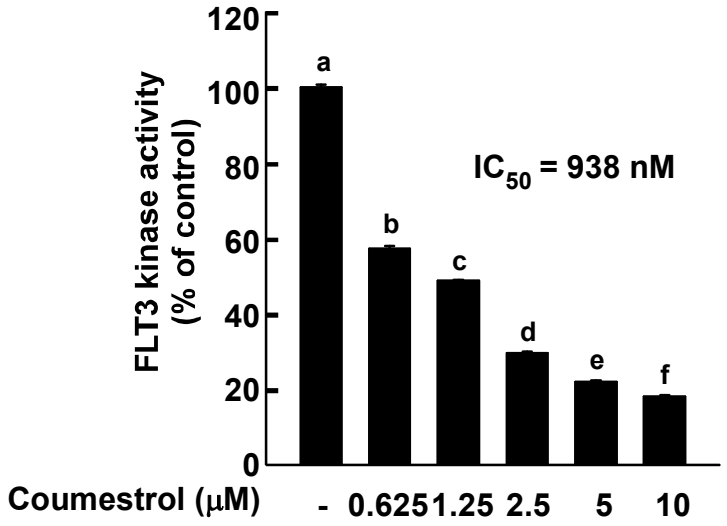

Figure 4. Effect of coumestrol on FLT3 kinase activity *in vitro*.

Coumestrol decreased FLT3 activity *in vitro* (IC_{50} = 938 nM). Kinase activity was analyzed in the presence or absence of coumestrol as described in the Materials and Methods. Data were shown as the means ± S.D. (n = 3).

3.4. Coumestrol decreases MMP-1 transcription by inhibiting Raf/MEK/ERK and Akt/p70S6K signaling pathways.

Based on the previous studies, FLT3 kinase is an upstream regulator of Raf/MEK/ERK and Akt/p70S6K signaling pathways [26-28]. MAPKs and Akt/p70S6 kinase have been shown to regulate MMP-1 expression [13, 14, 29]. Thus, I examined the effect of coumestrol on UVB-induced phosphorylation and total levels of these kinases in HDFs. In Fig. 5A - C, I confirmed that coumestrol inhibited UVB-induced phosphorylation of MEK/ERK and Akt/p70S6K in a dose-dependent manner. The alteration of these signal transduction cascades led to modulation of nuclear transcription factor AP-1 transactivation (Fig. 5D) and finally decreased MMP-1 mRNA transcription (Fig. 5E). These results indicated that coumestrol suppressed UVB-induced MMP-1 gene transcription by inhibiting AP-1 activity that was regulated by ERK- and Akt-mediated signaling pathways.

Figure 5

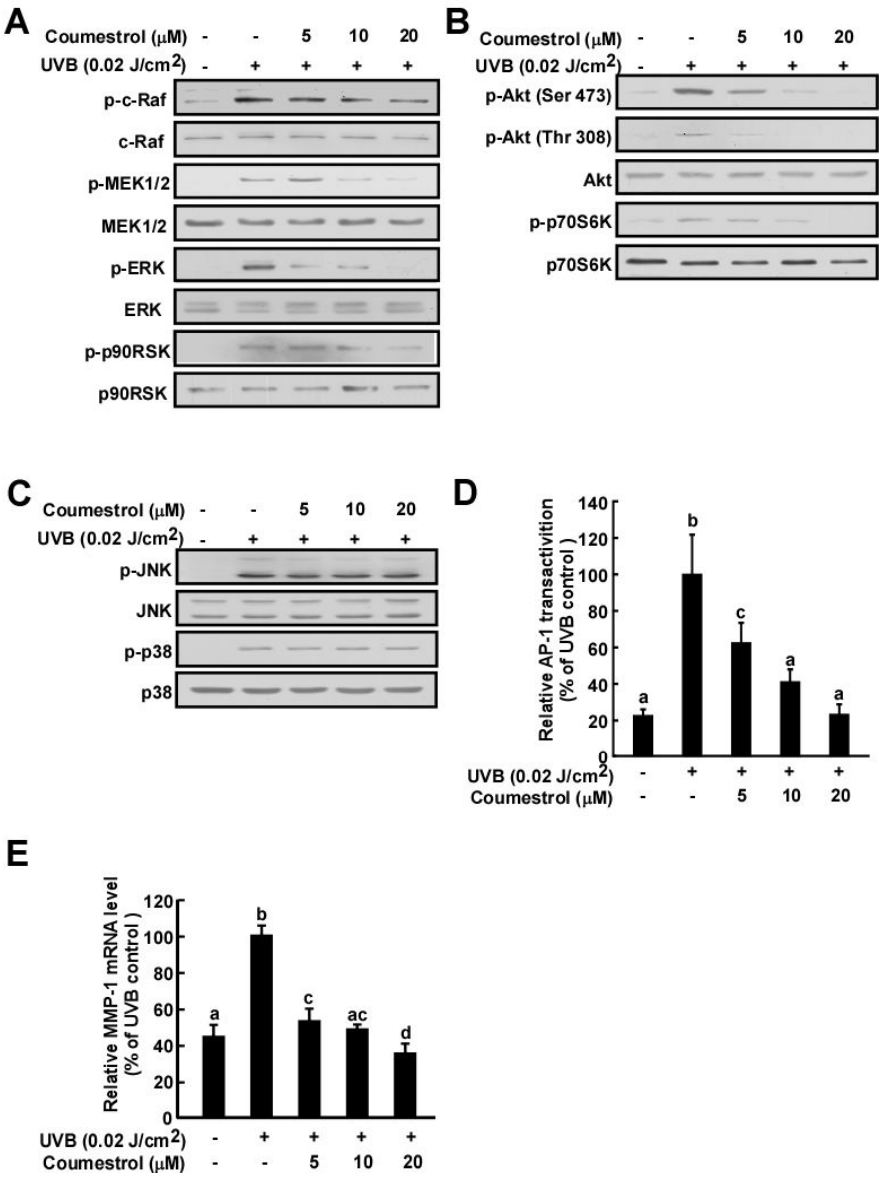
A
Coumestrol (μM) - - 5 10 20
UVB (0.02 J/cm2) - + + + +
p-c-Raf
c-Raf
p-MEK1/2
MEK1/2
p-ERK
ERK
p-p90RSK
p90RSK
B
Coumestrol (μM) - - 5 10 20
UVB (0.02 J/cm2) - + + + +
p-Akt (Ser 473)
p-Akt (Thr 308)
Akt
p-p70S6K
p70S6K
C
Coumestrol (μM) - - 5 10 20
UVB (0.02 J/cm2) - + + + +
p-JNK
JNK
p-p38
p38
D
Relative AP-1 transactivition (% of UVB control)
140
120
100
80
60
40
20
0
a
b
c
a
a
UVB (0.02 J/cm2) - + + + +
Coumestrol (μM) - - 5 10 20
E
Relative MMP-1 mRNA level (% of UVB control)
120
100
80
60
40
20
0
a
b
c
ac
d
UVB (0.02 J/cm2) - + + + +
Coumestrol (μM) - - 5 10 20

Figure 5. Inhibitory effect of coumestrol on UVB-induced signaling pathways.

A, Effect of coumestrol on UVB-induced Raf/MEK/ERK signaling pathway. After coumestrol treatment and UVB irradiation, the cells were lysed as described in the Materials and Methods. Phosphorylated and total form of indicated proteins was determined by Western blotting as described in the Materials and Methods. Total form of each protein was used as a loading control. **B** and **C**, Effect of coumestrol on MAPKs. Each of the phosphorylated- and total protein levels of indicated proteins was determined by Western blotting as described above. All data are representative of three independent experiments that gave similar results. **D**, AP-1 transactivation ability was measured using a Luciferase assay as described in the Materials and Methods. **E**, MMP-1 mRNA level of coumestrol was analyzed by Real-time RT-PCR. Data of **D** and **E** are the means ± S.D. (n = 3). Means with letters (a-d) within a graph were significantly different from each other at $p < 0.05$.

3.5. Inhibition of FLT3 kinase diminishes UVB-induced MMP-1 expression through ERK and Akt pathway.

To verify the involvement of FLT3 kinase in the UVB-induced MMP-1 expression, I blocked a FLT3 signaling pathway using a FLT3 specific inhibitor (4-APIA) [30] and identified changes of MMP-1 expression and signaling cascade in HDFs. 4-APIA inhibited UVB-induced MMP-1 expression (Fig. 6A). Moreover, 4-APIA reduced UVB-induced phosphorylation of ERK and Akt (Fig. 6B and C), but not JNK and p38. These results further confirms that targeting FLT3 kinase is key regulatory mechanism of coumestrol for inhibiting UVB-induced MMP-1 expression.

Figure 6

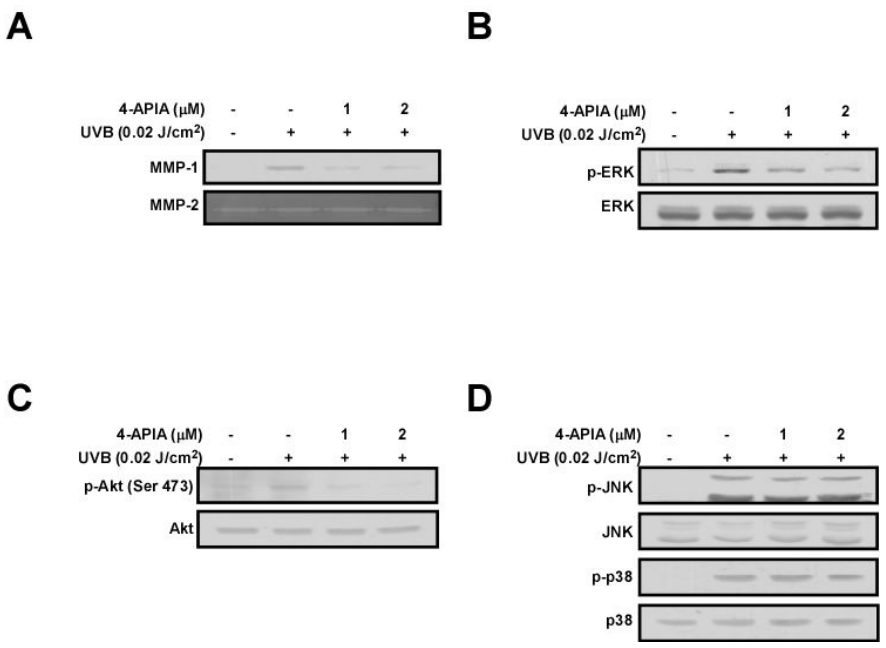

Figure 6. Both coumestrol and FLT3 inhibitor regulate MMP-1 expression by inhibiting ERK and Akt pathway.

A, The effect of 4-APIA on UVB-induced MMP-1 expression. After 1 h 4-APIA treatment, 0.02 J/cm^2 UVB was irradiated. The supernatants were collected after 2 days and MMP-1 expression was detected by Western blotting as described at Materials and

Methods. MMP-2 expression was used as loading control. **B**, The effect of 4-APIA on MAPKs and Akt phosphorylation. After 4-APIA treatment and UVB irradiation, the cells were lysed as described at Materials and Methods. Phosphorylation and total form of indicated proteins was determined by Western blotting as described at Materials and Methods. Total form of each protein was used as loading control. All data were representative of three independent experiments that gave similar results.

IV. Discussion

Sunlight is a major factor of triggering skin aging and we call this phenomenon as photoaging. Particularly, UVB is more energetic than the other sunlight, so it is regarded as a critical reason of photoaging and cause of furrow and sagging [5, 7]. These changes are caused by increased MMPs expression. Various MMPs including MMP-1 (collagenase), MMP-3 (stromelysine-1), and MMP-9 (gelatinase B) are increased in the human skin or dermal fibroblasts when they expose to UVB, but not induces MMP-2 (gelatinase A) [6, 9, 14]. MMP-1 initiates cleavage of fibrillar collagen to make triple helix coil into a single site [31]. Once collagen fibrils cleaved by MMP-1, collagen fiber can be further degraded by elevated levels of MMP-3 and MMP-9 [32]. So MMP-1 is regarded a main enzyme in deteriorating ECM degradation and wrinkle formation [33]. Accordingly, the prevention or inhibition of UVB-induced MMP-1 overexpression represent an effective strategy to ameliorate photoaging.

3D human skin equivalent is in the limelight these days,

because it mimics the morphology and physiology of human skin and might be the alternation of animal test. In order to overcome a limit of monolayer culture and test at the similar environment of actual skin, I used this method for measuring the anti-wrinkle effects of coumestrol.

In case of Koreans, more than 94 % of total isoflavone intake was attributable to soybeans and three traditional soy foods (tofu, soybean paste, soybean sprouts) and the average soy isoflavone consumption was approximately 15 mg/day (western people < 1 mg/day) [34]. When soybeans germinate or be infected, it synthesizes coumestrol autonomously from second metabolites of isoflavone through *de novo* synthesis [17, 18]. Koreans mostly get coumestrol from soybean sprout, and coumestrol intake is approximately 10 times greater in Asian women than non-Asian women [35]. Soy isoflavones are effective in improving wrinkle formation and skin elasticity [36]. This study indicate that coumestrol exhibit better inhibitory effect on MMP-1 transcription than daidzin and daidzein at the same dose (20 μM).

UV irradiation leads reactive oxygen species (ROS) generation or activates membrane receptors of fibroblasts and keratinocytes, and then transmits to signaling pathway to promote MMP-1 expression [37, 38]. Many previous studies have proposed that the advantage of phytochemicals comes from ROS scavenging effects [39]. However, most of these hypothesizes could not explain their specific inhibition effects of signaling transduction and the low effective dose. Therefore, modulating the direct targets of phytochemical can explain the strong bioactivity of various phytochemicals at low concentration and treatment on alternative signaling pathways. I therefore focus on identifying the molecular target of coumestrol, and then confirm its inhibitory effect on downstream effectors and treatment outcomes as a result of binding.

FMS-like tyrpsine kinase 3 (FLT3) is one of the tyrosine kinase receptor (RTK), which belongs to the class III RTK family including stem cell factor (SCF) receptor (c-Kit), macrophage colony-stimulating factor (M-CSF) receptor (FMS) and platelet derived growth factor receptor A and B (PDGFRA and PDGFRB)

[40]. During UVB irradiation, FLT3 ligand (FL), such as SCF, c-kit and so on, are elevated [41], after that FLT3 ligand (FL) binds to extracellular portion of FLT3. FLT3 forms homodimer and initiates phosphorylation of Ras/MEK/ERK pathway and PI3K/Akt pathway. Also FLT3 can automatically phosphorylate and start FLT3 pathway [26-28]. Therefore, the effect of coumestrol on UVB-induced FLT3 pathway has been investigated in this study.

Phosphorylation of MAPKs, which consists of extracellular signal-regulated kinase (ERK), c-Jun N-terminal kinase (JNK), and p38, promotes expression or activation of AP-1 [13]. Among them, coumestrol downregulates only ERK phosphorylation level. This influence is caused by the inhibitory effect of coumestrol on c-Raf phosphorylation. Also as a result of checking on the PI3K/Akt pathway, coumestrol suppresses Akt/p70 ribosomal S6 kinase (p70S6K) phosphorylation. It is widely known that PI3K and its downstream target p70S6K are critically related to the UVB-inducted MMP-1 and MMP-3 expression in fibroblasts [14]. Moreover serine/ threonine protein kinase Akt (also known as

protein kinase B, PKB), downstream effector of PI3K, activated by UVB [29, 42] and Akt/p70S6 Kinase signal cascade is subsequently stimulated. Finally phosphorylated Akt increases transcription of genes for MMP-1, MMP-3, and MMP-9 through up-regulated AP-1 activity [14, 43, 44]. All things taken together, coumestrol regulates FLT3 signaling pathway. For these influences, elevated levels of AP-1 activity are decreased and MMP-1 gene transcription is inhibited. In addition, when I block the FLT3 pathway using pharmacological inhibitor 4-APIA, I could confirm that the regulatory mechanisms of UVB-induced MMP-1 expression is similar to coumestrol.

In conclusion, the novel role of coumestrol in wrinkle formation has been discovered through regulating MMP-1 transcription which involves decreased AP-1 activity by targeting FLT3 kinase resulting in suppression of Ras/MEK/ERK and Akt/p70S6K pathway. Also I find out that an anti-photoaging effect of coumestrol is superior to its precursors (daidzin and daidzein). Moreover, I establish the relationship between MMP-1 expression

and FLT3 pathway for the first time. In further study, X-ray crystallography and clinical studies should be performed. Coumestrol could be used as a beneficial agent in preventing photoaging and the FLT3 kinase would be an outstanding therapeutic target of wrinkle formation.

V. References

1. Yaar, M. and B.A. Gilchrest, Photoageing: mechanism, prevention and therapy. Br J Dermatol, 2007. **157**(5): p. 874-87.
2. Jenkins, G., Molecular mechanisms of skin ageing. Mech Ageing Dev, 2002. **123**(7): p. 801-10.
3. Chung, J.H., Photoaging in Asians. Photodermatol Photoimmunol Photomed, 2003. **19**(3): p. 109-21.
4. UITTO, J., Understanding premature skin aging. The New England Journal of Medicine, 1997. **337**.
5. Yaar, M., Clinical and histological features of intrinsic versus extrinsic skin aging. 2006: Springer.
6. Brenneisen, P., H. Sies, and K. Scharffetter-Kochanek, Ultraviolet-B irradiation and matrix metalloproteinases: from induction via signaling to initial events. Ann N Y Acad Sci, 2002. **973**: p. 31-43.
7. Matsumura, Y. and H.N. Ananthaswamy, Toxic effects of ultraviolet radiation on the skin. Toxicol Appl Pharmacol,

2004. **195**(3): p. 298-308.

8. Biniek, K., K. Levi, and R.H. Dauskardt, Solar UV radiation reduces the barrier function of human skin. Proc Natl Acad Sci U S A, 2012. **109**(42): p. 17111-6.

9. Fisher, G.J., et al., Molecular basis of sun-induced premature skin ageing and retinoid antagonism. Nature, 1996. **379**(6563): p. 335-9.

10. GJ, F., et al., PATHOPHYSIOLOGY OF PREMATURE SKIN AGING INDUCED BY ULTRAVIOLET LIGHT. N Engl J Med, 1997. **1997**(337): p. 20.

11. Uitto, J., M.J. Fazio, and D.R. Olsen, Molecular mechanisms of cutaneous aging. Age-associated connective tissue alterations in the dermis. J Am Acad Dermatol, 1989. **21**(3 Pt 2): p. 614-22.

12. JH, C., et al., Modulation of Skin Collagen Metabolism in Aged and Photoaged Human Skin In Vivo. J Invest Dermatol, 2001. **117**(5): p. 1218-1224.

13. Whitmarsh, A.J. and R.J. Davis, Transcription factor AP-1 regulation by mitogen-activated protein kinase signal

transduction pathways. J Mol Med (Berl), 1996. **74**(10): p. 589-607.

14. Brenneisen, P., Activation of p70 Ribosomal Protein S6 Kinase Is an Essential Step in the DNA Damage-dependent Signaling Pathway Responsible for the Ultraviolet B-mediated Increase in Interstitial Collagenase (MMP-1) and Stromelysin-1 (MMP-3) Protein Levels in Human Dermal Fibroblasts. Journal of Biological Chemistry, 2000. **275**(6): p. 4336-4344.

15. AL, M., W. G, and D. SR, Phytoestrogens. Journal of Clinical Endocrinology and Metabolism, 1998. **83**(2): p. 297-303.

16. Simons, R., et al., Prenylated isoflavonoids from plants as selective estrogen receptor modulators (phytoSERMs). Food Funct, 2012. **3**(8): p. 810-27.

17. Simons, R., et al., Identification of prenylated pterocarpans and other isoflavonoids in Rhizopus spp. elicited soya bean seedlings by electrospray ionisation mass spectrometry. Rapid Commun Mass Spectrom, 2011. **25**(1): p. 55-65.

18. Kurosu, M., Soybean and Health: Biologically Active Molecules from Soybeans. InTech, 2011. **10**.

19. Yuk, H.J., et al., The most abundant polyphenol of soy leaves, coumestrol, displays potent α-glucosidase inhibitory activity. Food Chemistry, 2011. **126**(3): p. 1057-1063.

20. Jeon, H.Y., et al., Effect of Aspergillus oryzae-challenged germination on soybean isoflavone content and antioxidant activity. J Agric Food Chem, 2012. **60**(11): p. 2807-14.

21. LEE, J.H., et al., LDL-antioxidant pterocarpans from roots of Glycine max (L.) Merr. J Agric Food Chem, 2006. **54**(6): p. 2057-2063.

22. Canal Castro, C., et al., Coumestrol has neuroprotective effects before and after global cerebral ischemia in female rats. Brain Res, 2012. **1474**: p. 82-90.

23. Lee, Y.H., et al., Coumestrol induces senescence through protein kinase CKII inhibition-mediated reactive oxygen species production in human breast cancer and colon cancer cells. Food Chem, 2013. **141**(1): p. 381-8.

24. Taxvig, C., et al., Dietary relevant mixtures of

phytoestrogens inhibit adipocyte differentiation in vitro. Food Chem Toxicol, 2013. **55**: p. 265-71.

25. Uhlen, M., et al., Towards a knowledge-based Human Protein Atlas. Nat Biotechnol, 2010. **28**(12): p. 1248-50.

26. Dosil, M., S. Wang, and I.R. Lemischka, Mitogenic signalling and substrate specificity of the Flk2/Flt3 receptor tyrosine kinase in fibroblasts and interleukin 3-dependent hematopoietic cells. Molecular and cellular biology, 1993. **13**(10): p. 6572-6585.

27. Takahashi, S., Inhibition of the MEK/MAPK signal transduction pathway strongly impairs the growth of Flt3-ITD cells. American journal of hematology, 2006. **81**(2): p. 154-155.

28. Takahashi, S., Downstream molecular pathways of FLT3 in the pathogenesis of acute myeloid leukemia: biology and therapeutic implications. J Hematol Oncol, 2011. **4**: p. 13.

29. Ibuki, Y. and R. Goto, Suppression of apoptosis by UVB irradiation: survival signaling via PI3-kinase/Akt pathway. Biochemical and biophysical research communications,

2000. **279**(3): p. 872-878.

30. Dai, Y., et al., Discovery of N-(4-(3-amino-1H-indazol-4-yl)phenyl)-N'-(2-fluoro-5-methylphenyl)urea (ABT-869), a 3-aminoindazole-based orally active multitargeted receptor tyrosine kinase inhibitor. J Med Chem, 2007. **50**(7): p. 1584-97.

31. GJ, F., et al., Mechanisms of Photoaging and Chronological Skin Aging. Arch Dermatol, 2002. **138**(11): p. 1462-1470.

32. Sternlicht, M.D. and Z. Werb, How matrix metalloproteinases regulate cell behavior. Annu Rev Cell Dev Biol, 2001. **17**: p. 463-516.

33. Brennan, M., et al., Matrix metalloproteinase-1 is the major collagenolytic enzyme responsible for collagen damage in UV-irradiated human skin. Photochem Photobiol, 2003. **78**(1): p. 43-8.

34. Kim, J. and C. Kwon, Estimated dietary isoflavone intake of Korean population based on National Nutrition Survey. Nutr Res, 2001. **21**(7): p. 947-953.

35. Surh, J., et al., Estimated intakes of isoflavones and

coumestrol in Korean population. Int J Food Sci Nutr, 2006. **57**(5-6): p. 325-44.

36. T, I., et al., Oral intake of soy isoflavone aglycone improves the aged skin of adult women. J Nutr Sci Vitaminol (Tokyo), 2007. **53**(1): p. 57-62.

37. Chen, L., J.Y. Hu, and S.Q. Wang, The role of antioxidants in photoprotection: a critical review. J Am Acad Dermatol, 2012. **67**(5): p. 1013-24.

38. Rittié, L. and G.J. Fisher, UV-light-induced signal cascades and skin aging. Ageing Research Reviews, 2002. **1**: p. 705-720.

39. Di Carlo, G., et al., Flavonoids: old and new aspects of a class of natural therapeutic drugs. Life Sci, 1999. **65**(4): p. 337-53.

40. Stirewalt, D.L. and J.P. Radich, The role of FLT3 in haematopoietic malignancies. Nat Rev Cancer, 2003. **3**(9): p. 650-65.

41. Hachiya, A., et al., The Paracrine Role of Stem Cell Factor/c-kit Signaling in the Activation of Human

Melanocytes in Ultraviolet-B-Induced Pigmentation. Journal of Investigative Dermatology, 2001. **116**: p. 578–586.

42. Kuhn, C., et al., Activation of the insulin-like growth factor-1 receptor promotes the survival of human keratinocytes following ultraviolet B irradiation. Int J Cancer, 1999. **80**(3): p. 431-8.

43. Oh, J.H., et al., Ultraviolet B-induced matrix metalloproteinase-1 and -3 secretions are mediated via PTEN/Akt pathway in human dermal fibroblasts. J Cell Physiol, 2006. **209**(3): p. 775-85.

44. Angel, P., A. Szabowski, and M. Schorpp-Kistner, Function and regulation of AP-1 subunits in skin physiology and pathology. Oncogene, 2001. **20**(19): p. 2413-23.

Ⅵ. 국문초록

피부노화는 자연적으로 일어나는 현상이지만, 자외선 노출로 과다하게 발현되는 콜라겐분해효소(MMP-1)에 의하여 주름 형성 및 탄력 저하가 가속화된다. 본 연구는 콩 유래 아이소플라본인 다이드진으로부터 신생합성되는 쿠메스트롤의 자외선에 의한 피부노화를 예방하는 효능에 대하여 규명하였다. 쿠메스트롤은 UVB에 의해 촉진되는 MMP-1의 활성을 농도 의존적으로 억제하였으며, 이는 MMP-1의 전사과정이 저해됨으로써 기인함을 밝혔다. 전사과정을 조절하는 상위 신호전달 표적 단백질을 찾기 위하여 Kinase profiling analysis와 Kinase assay를 수행하였으며, 쿠메스트롤이 FLT3 활성을 억제하는 것을 확인하였다. 또한 쿠메스

트롤은 Ras/MEK/ERK 및 Akt/p70S6K의 인산화를 억제하여 MMP-1 전사인자인 AP-1의 활성을 저해하였다. 4-APIA를 이용하여 FLT3 활성을 억제하였을 때에도 MMP-1의 발현이 감소되고, 쿠메스트롤과 유사한 신호전달 변화가 나타남을 확인하였다. 본 연구 결과, 쿠메스트롤이 UVB에 의한 FLT3 활성을 직접적으로 억제하여 하위 신호전달 변화로 인해 MMP-1 전사과정이 저해됨을 규명하였으며, 이를 통하여 자외선 노출로 인한 피부노화를 개선하는 신규 천연물로서 쿠메스트롤의 가능성을 제시하였다.

주요어: 쿠메스트롤; 에프엠에스-라이크 타이로신 카이네이즈 3; 메트릭스 메탈로프로테이네이즈-1; 자외선